OXFORD

Research Article

Augmented H$_2$S production via cystathionine-beta-synthase upregulation plays a role in pregnancy-associated uterine vasodilation[†]

Lili Sheibani[1,‡], Thomas J. Lechuga[1,‡], Honghai Zhang[1], Afshan Hameed[1], Deborah A. Wing[1], Sathish Kumar[2], Charles R. Rosenfeld[3] and Dong-bao Chen[1,*]

[1]Department of Obstetrics and Gynecology, University of California Irvine, Irvine, California, USA; [2]Department of Obstetrics and Gynecology, University of Texas Medical Branch-Galveston, Galveston, Texas, USA and [3]Department of Pediatrics and Obstetrics and Gynecology, University of Texas Southwestern Medical School, Dallas, Texas, USA

*Correspondence: Department of Obstetrics and Gynecology, University of California Irvine, 140A Medical Surge 1, Irvine, CA 92697, USA. E-mail: dongbaoc@uci.edu.

Abstract

Endogenous hydrogen sulfide (H$_2$S) synthesized via metabolizing L-cysteine by cystathionine-beta-synthase (CBS) and cystathionine-gamma-lyase (CSE) is a potent vasodilator and angiogenic factor. The objectives of this study were to determine if human uterine artery (UA) H$_2$S production increases with augmented expression and/or activity of CBS and/or CSE during the menstrual cycle and pregnancy and whether exogenous H$_2$S dilates UA. Uterine arteries from nonpregnant (NP) premenopausal proliferative (pPRM) and secretory (sPRM) phases of the menstrual cycle and pregnant (P) women were studied. H$_2$S production was measured by the methylene blue assay. CBS and CSE mRNAs were assessed by quantitative real-time PCR, and proteins were assessed by immunoblotting and semiquantitative immunofluorescence microscopy. Effects of H$_2$S on rat UA relaxation were determined by wire myography *ex vivo*. H$_2$S production was greater in NP pPRM and P than NP sPRM UAs and inhibited by the specific CBS but not CSE inhibitor. CBS but not CSE mRNA and protein were greater in NP pPRM and P than NP sPRM UAs. CBS protein was localized to endothelium and smooth muscle and its levels were in a quantitative order of P >NP UAs of pPRM>sPRM. CSE protein was localized in UA endothelium and smooth muscle with no difference among groups. A H$_2$S donor relaxed P > NP UAs but not mesentery artery. Thus, human UA H$_2$S production is augmented with endothelium and smooth muscle CBS upregulation, contributing to UA vasodilation in the estrogen-dominant physiological states in the proliferative phase of the menstrual cycle and pregnancy.

Summary Sentence

Augmented hydrogen sulfide biosynthesis via upregulating endothelium and smooth muscle cystathionine β-synthase expression plays a role in pregnancy-associated uterine vasodilation.

Introduction

During pregnancy, eutherian mammals, including humans, must make a series of changes in the body to accommodate the metabolic demands of the developing fetus [1]. Notably, the mother's cardiovascular system makes a number of adaptive changes, including increased blood volume and cardiac output, systemic vasodilation, and decreased vascular resistance with no change or slight decrease in blood pressure, etc. [2]. These changes force a redistribution of cardiac output to reproductive organs, especially the uterus, such that a substantially increased volume of blood is delivered to the maternal–fetal interface. For instance, in nonpregnant (NP) ewes less than 1%–2% of cardiac output is distributed to the reproductive organs and this number increases to $\sim$15%–20% in late pregnant (P) ewes, with the largest portion ($>$95%) directed to the rapidly developing uteroplacental vascular bed, as reflected by a striking rise in uterine blood flow (UBF) from $\sim$10 mL/min to as high as $\sim$500–800 mL/min in NP vs. P ewes [2]. The rise in UBF facilitates the bidirectional maternal–fetal exchange of gases (O_2 and CO_2) and provides the sole source of nutrients to support fetal and placental growth, making UBF a critical rate-limiting factor for pregnancy health. Constrained UBF results in intrauterine growth restriction, preeclampsia, and other pregnancy disorders [3–5], as well as long-term effects in the mother and newborns [6].

Pregnancy-associated uterine vasodilation has been linked to significantly augmented local production of orchestrated networks of vasodilator substances, including prostacyclin [7, 8], nitric oxide (NO) [9], endothelium-derived hyperpolarizing factor (EDHF) [10], vascular endothelial growth factor A (VEGFA) [11], etc. Among them, endothelium NO production via endothelial NO synthase 3 (NOS3) activation and/or expression [12–14] is a key player in pregnancy-augmented uterine vasodilation because (1) enhanced NOS3 expression mediates pregnancy-augmented endothelium/NO-dependent human uterine artery (UA) dilator responses to acetylcholine [15, 16] and (2) NOS3/NO is important for vascular remodeling, decreased vascular resistance, increased blood flow, and pregnancy outcomes [17, 18]. Moreover, NOS3/NO appears to function as a focal mediator as it interacts with nearly all known vasodilators, including EDHF and VEGFA [10, 11, 19]. However, prolonged UA NOS inhibition only modestly alters baseline uteroplacental vasodilation in the last one third of ovine pregnancy [20], suggesting that mechanisms in addition to NO exist.

Hydrogen sulfide (H_2S) has now been accepted as the third "gasotransmitter" after NO and carbon monoxide due to its NO-like biological properties [21–23]. Endogenous H_2S is mainly synthesized by two key enzymes cystathionine-beta-synthase (CBS) and cystathionine-gamma-lyase (CSE) [24, 25]. These enzymes produce H_2S from L-cysteine, CBS via a beta-replacement reaction with a variety of thiols, and CSE by disulfide elimination followed by reaction with various thiols [24, 25]. H_2S can be also synthesized via 3-mercaptopyruvate sulfurtransferase (3MST), cytosolic cysteine aminotransferase (cCAT), and mitochondrial cysteine aminotransferase (mCAT), but to a much less extent [26]. In mammals, H_2S potently dilates various vascular beds via activating ATP-dependent potassium (K_{ATP}) channel [27] and relaxes smooth muscle via activating large conductance calcium-activated potassium (BK_{Ca}) channel [28]. H_2S also promotes angiogenesis in vitro and in vivo [29]. Thus, H_2S functions as a potent vasodilator [30]. Recent studies also highlight a role of CSE/H_2S in placental development and function as well as pregnancy because (1) H_2S potently dilates placental vasculature [31] and (2) dysregulation of CSE expression results in maternal hypertension and placental abnormalities in preeclampsia [32]. However, whether pregnancy regulates H_2S biosynthesis in maternal uterine and systemic vasculatures and whether H_2S plays a role in pregnancy-associated uterine and systemic vasodilation have not been reported to date.

We recently reported first that the H_2S biosynthesis system is present in the UA, which is significantly stimulated by exogenous estrogen replacement therapy via selectively upregulating CBS expression in ovariectomized NP ewes [33]. However, it is unknown whether endogenous estrogens regulate UA H_2S system. Thus, we hypothesized here that UA H_2S biosynthesis is augmented in human UA during estrogen-"dominant" physiological states: that is, the proliferative phase of the menstrual cycle and pregnancy, and that H_2S plays a role in uterine vasodilation. The specific objectives of the study were to determine whether (1) CBS and/or CSE activities are greater in UAs during estrogen-dominant physiological states in women; (2) the changes in UA CSE and CBS activities are associated with increases in their mRNA/protein expression; (3) enhanced CBS and/or CSE proteins are located in the vascular endothelium or smooth muscle cells; and (4) H_2S donor regulates pregnancy-dependent uterine vasodilation.

Materials and methods

Human subjects and tissue collection

Primary UA samples were collected from 8 NP and 10 P women who underwent clinically indicated hysterectomy at the University of California Irvine Medical Center. Written consent was obtained from all participants, and ethical approval was granted from the University of California Irvine Institutional Review Board (HS#2013-9763) for Human Research. Twelve UA samples were collected from NP women with written consent, approved by the Institutional Review Board for Human Research at the University of Texas Southwestern Medical Center at Dallas. The 20 premenopausal NP women were at age 35–50 years old, undergoing elective hysterectomy are for fibroids (10 cases), abnormal uterine bleeding (9 cases), and pelvic organ prolapse (1 case). Menstrual status was determined by the last menstrual period recorded and confirmed with endometrial histology. Among them, 10 were in the proliferative and secretory phase, respectively. None were on hormone replacement therapy at the time of tissue collection. Pregnant subjects were recruited with suspected placental accreta based on previous ultrasound findings in the event a hysterectomy was indicated. Primary UAs were obtained from 10 P women of 35–36 weeks gestation at age 35–44. Both main UAs were dissected from the parametrium and paracervical tissues and adjacent myometrium, placed in chilled DMEM, and transported to the laboratory where they were placed in iced DMEM and the adventitia removed. Uterine artery segments ($\sim$1 cm long) were fixed

in 4% paraformaldehyde and the rest was frozen in liquid nitrogen, and stored at –80°C until analyzed.

Chemicals and antibodies

Monoclonal antibody against human CBS was from Abcam (Cambridge, MA). Monoclonal antibodies against human CSE, NOS3, 3MST, cCAT, and mCAT were from Santa Cruz Biotechnology (Dallas, TX). Anti-CD31 antibody was from Dako (Carpinteria, CA). Anti-beta-actin monoclonal antibody was from Ambion (Austin, TX). Prolong Gold antifade reagent with 4, 6-diamidino-2-phenylindole (DAPI), Alexa[488] and Alexa[568] conjugated goat anti-mouse immunoglobulin G (IgG) were from Invitrogen (Carlsbad, CA). Horseradish peroxidase-conjugated goat anti-mouse IgG was from Cell Signaling (Beverly, MA). GYY4137 and beta-cyano-L-alanine (BCA: inhibitor of CSE) were from Cayman Chemical (Ann Arbor, MI). O-(Carboxymethyl)hydroxylamine hemihydrochloride (CHH: inhibitor of CBS) and all other chemicals unless specified were from Sigma (St. Louis, MO).

Methylene blue assay

Tissue H_2S production was determined by the methylene blue assay as previously described [33], with minor modifications. Briefly, segments of frozen intact UA tissue were homogenized in ice-cold 50 mM potassium phosphate buffer, pH 8. The reaction mixture contained: 50 mM potassium phosphate buffer pH 8.0, 10 mM L-cysteine, and 2 mM pyridoxal 5′-phosphate. Microtubes (2 mL) were used as the center wells; each contained 0.3 mL of 1% zinc acetate as trapping solution and a filter paper of 0.5×1.5 cm to increase the air/liquid contacting surface. The reaction was performed in 12 ml test tubes. The tubes containing the reaction mixture and center wells were flushed with N_2 before being sealed with a double layer of Parafilm. The reaction was initiated by transferring the tubes from ice to a 37°C shaking water bath. After incubating at 37°C for 90 min, the reaction was stopped by adding 0.5 mL of 50% trichloroacetic acid. The tubes were sealed again and incubated at 37°C for another 60 min to ensure a complete trapping of the H_2S released from the mixture. Subsequently, 0.05 mL of 20 mM N, N-dimethyl-p-phenylenediamine sulfate in 7.2 M HCl was added immediately after the addition of 0.05 mL 30 mM $FeCl_3$ in 1.2 M HCl. The absorbance of the resulting solution at 670 nm was measured after 20 min. The H_2S concentration was calculated based on a calibration curve generated from NaHS solutions. For CBS and CSE inhibition experiments, their respective inhibitor CHH or BCA was added separately or in combination (final conc. = 2 mM) to the reaction mixtures prior to initiating the methylene blue assay.

RNA extraction, reverse transcription, and real-time qPCR

Total RNAs were extracted from intact UA segments using Trizol reagent (Invitrogen, Carlsbad, CA) following the manufacturer's instructions. RNA was quantified by $OD_{260/280}$. Complementary DNA (cDNA) was synthesized by reverse transcription with random primers and AMV Reverse Transcriptase (Promega, Madison, WI). The cDNAs were used for quantifying CBS and CSE mRNAs by quantitative real-time PCR (run in triplicate) with gene-specific primers exactly as detailed previously [33]. Briefly, each real-time PCR reaction contained 7.5 μL of RT^2 Real-Time PCR SYBR Green master mix (SABiosciences), 10 μM forward and reverse primers, 3 μL of cDNA template in with 15 μL final volume in nuclease-free H_2O. A StepOnePlus Real-Time PCR system (Life Technologies,

Grand Island, NY) was used with a three-step thermal cycling program: initial denaturing at 95°C for 10 min, followed by 40 cycles of 95°C for 15 s, 55°C for 30 s, and 72°C for 30 s, and a melting curve program (95°C, 15 s; 60°C, 1 min, optics off; 60°C to 95°C at 2°C/min, optics on). Comparative C_T method ($\Delta\Delta C_T$ method) was used to calculate relative CBS and CSE mRNA levels with the use of ribosomal protein L19 as the internal reference control.

Sodium dodecyl sulfate polyacrylamide gel electrophoresis (SDS-PAGE) and western blot analysis

Protein extracts were prepared from homogenates of artery segments in a nondenaturing buffer containing protease cocktail [33]. Protein concentrations were determined by using the Pierce BCA Protein Assay Kit (Pierce Biotechnology, Rockford, IL). Proteins (15 μg/sample) were separated on 10% SDS-PAGE and transferred onto polyvinylidene fluoride membranes. The membranes were subjected to immunoblotting with mouse monoclonal antibodies (0.4 μg/mL) of human CBS, CSE, NOS3, 3MST, cCAT, or mCAT, followed by horseradish peroxidase-conjugated goat anti-mouse IgG (0.01 μg/mL). Bound antibodies on membranes were visualized by using the SuperSignal West Femto Maximum Sensitivity Substrate (Thermo Fisher Scientific, Waltham, MA), and digital images were captured using a ChemiImager Imaging System (Alpha Innotech, San Leandro, CA). The membranes were striped and reprobed with mouse anti-beta-actin antibody (0.1 μg/mL) for normalizing sample loading. Immunoreactive bands of CBS and CSE proteins were quantified by NIH *Image*J software and presented as fold changes over premenopausal proliferative phase of the menstrual cycle (pPRM).

Immunofluorescence microscopy and image analysis

The cellular specific expression of CBS and CSE proteins in human UA was determined by immunofluorescence microscopy. Sections were *de*paraffinized in xylene, and rehydrated by passing through gradient ethanol. Sections were incubated in 0.05% trypsin to unmask antigens at room temperature for 30 min. Autofluorescence was quenched by washing the sections with 300 mM glycine in phosphate-buffered saline (PBS; 3×20 min); nonspecific binding was blocked by incubating with PBS containing 1% BSA, 0.125% saponin, and 1% gelatin at room temperature for 30 min. Sections were then incubated with anti-CD31 (5 μg/mL) overnight at 4°C. Following three 5-minute washes in PBS, the sections were then incubated with Alexa[568] conjugated goat anti-mouse IgG (2 μg/mL) at room temperature for 1 h. Following three 20-min washes in PBS, sections were then incubated with 1 μg/mL of anti-CBS or anti-CSE antibodies at room temperature for 2 h, followed by incubation with Alexa[488] conjugated donkey anti-rabbit IgG or goat anti-mouse IgG (2 μg/mL) at room temperature for 1 h. Following three 20-min PBS washes, the sections were mounted with Prolong Gold antifade reagent (Invitrogen) containing DAPI for labeling cell nuclei.

Samples were examined under a Leica fluorescence microscope (Leica Corporation, Deerfield, IL), and digital images were acquired using a charge-coupled device camera with the *Simple*PCI image analysis software (Hamamatsu Corporation, Sewickley, PA). The images were used to determine relative levels of CBS and CSE proteins by quantifying mean green fluorescence intensity using *Simple*PCI image analysis software. For all groups, CBS and CSE levels were averaged from data collected from five to six images per subject, and three to four subjects per group. Intima and media areas were outlined using the "Region of Interest" selection tool and "Mean Green Value" was recorded for a cell. The average "Mean Green

Value" from negative control sections without primary antibody accounted for autofluorescence and nonspecific background, which was subtracted from all counts generated from specific antibody-treated samples. CBS and CSE protein levels were presented as fold change in the average fluorescence intensity.

Animals and wire myography studies

Sprague Dawley rats from Charles River (Wilmington, MA) were used in the experiment. All experimental procedures were in accordance with National Institutes of Health guidelines (NIH Publication No. 85–23, revised 1996) with approval by the Animal Care and Use Committee at the University of Texas Medical Branch at Galveston. Adult diestrous NP and timed P (day 20) rats were sacrificed by CO_2 asphyxiation. Primary UA and secondary mesenteric arteries (MA) were dissected under a dissecting microscope and placed directly into ice-cold Krebs buffer (in mM: NaCl, 119; KCl, 4.7; $CaCl_2$, 2.5; $MgSO_4$, 1.17; $NaHCO_3$, 25; KH_2PO_4, 1.18; EDTA, 0.026; and d-glucose, 5.5; pH 7.4). Uterine and mesenteric arteries were cut into 1.5–2 mm segments and mounted between an isometric force transducer and a displacement device on a Multi Wire Myograph System (Model 620M; Danish Myo Technology) using two stainless steel wires (diameter 25 μm) for isometric tension recording, as previously described [34]. The myograph organ bath (6 mL) was filled with Krebs buffer maintained at 37°C and aerated with 95% O_2–5% CO_2. The vessels were washed and incubated for 30 min before performing the normalization procedure. Each arterial segment was stretched in a stepwise manner and the internal circumference and corresponding wall tension at each stretch were calculated and plotted to produce a resting wall tension-internal circumference curve for that particular artery using the normalization software (Powerlab, ADInstruments, Colorado Springs, CO). Uterine and mesenteric artery segments were normalized to 0.9 of L13.3kPa. After a 30-min equilibration period, arterial preparations were exposed to 1 μM phenylephrine until reproducible and maximal depolarization-induced constrictions were achieved. The presence of intact endothelium in the vascular preparations was confirmed by observing the relaxation response to 1 μM acetylcholine in rings preconstricted with phenylephrine. A cumulative concentration-response curve of GYY4137 was generated in rings preconstricted with submaximal phenylephrine concentrations. The relaxation responses were calculated as percent inhibition of phenylephrine-induced constriction; the pD₂ values (negative logarithm of molar concentration) of GYY4137 that produced 50% of the maximal tension for each vessel tested were calculated accordingly.

Statistical analysis

Data are presented as means ± SEM and analyzed by one-way or two-way analysis of variance (ANOVA), followed by the *Bonferroni* test for multiple comparisons using *Sigma*Stat (Systat Software Inc.). Significance was defined as $P < 0.05$, unless indicated in the figure legends.

Results

Uterine artery H₂S production in human menstrual cycle and pregnancy

Baseline H₂S production by NP secretory proliferative phase of the menstrual cycle (sPRM) and P UAs had 0.47 ± 0.17 and 2.60 ± 0.16-fold changes than NP sPRM and pPRM UAs, respectively
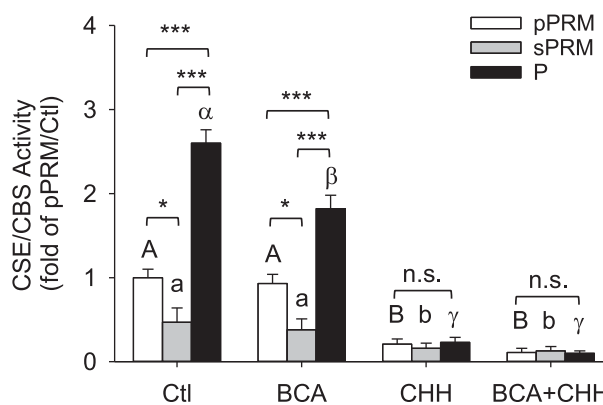

Figure 1. Effects of the menstrual cycle and pregnancy on H₂S production in human UAs. Protein lysates of intact UAs were subjected to the methylene blue assay for measuring H₂S production in the presence or absence of the specific inhibitors of CSE (BCA), CBS (CHH), or their combination. pPRM and sPRM: proliferative and secretory phases of the menstrual cycle; P: pregnancy. Data (mean ± SEM) are presented as fold of pPRM without inhibitors and are from 10 subjects per group. Bars with different letters differ significantly among the groups ($P < 0.05$). *$P < 0.05$; ***$P < 0.001$; n.s., not statistically different.

($P < 0.05$, Figure 1). Addition of the specific CSE inhibitor BCA reduced baseline H₂S production in intact UA lysates from P UA only. Addition of the specific CBS inhibitor CHH, inhibited baseline H₂S production in intact UA lysates from all three groups, especially in the pregnant ones. The combination of CHH plus BCA also inhibited NP baseline and pregnancy-augmented H₂S production, but this did not differ from CHH alone. Although BCA alone significantly change pregnancy-augmented H₂S production compared to that of NP UAs, CHH alone was able to attenuate pregnancy-augmented H₂S production. The combination of CHH and BCA significantly reduced NP baseline and pregnancy-augmented UA H₂S production. These data show that although both CBS and CSE contribute to baseline H₂S production, CBS is the major enzyme responsible for pregnancy-augmented H₂S biosynthesis in human UA.

Uterine artery cystathionine-beta-synthase and cystathionine-gamma-lyase mRNA and protein expression in human menstrual cycle and pregnancy

Levels of CBS mRNA in NP sPRM and P UAs had 0.43 ± 0.14 and 5.97 ± 0.73-fold changes ($P < 0.001$) than that in NP pPRM, respectively, and significantly differed from each other. In contrast, levels of UA CSE mRNA did not differ among the three groups ($P > 0.1$, Figure 2). Consistent with these findings, levels of CBS protein in NP sPRM and P UAs had 0.72 ± 0.18 and 2.62 ± 0.34-fold changes ($P < 0.001$; Figure 3) than that of NP pPRM UA and also were greater in P vs. NP sPRM. Levels of UA CSE protein did not differ among the three groups. We also confirmed NOS3 protein to be significantly upregulated in pPRM NP and P vs. sPRM NP UAs (Figure 3), consistent with previous reports [16]. In addition, 3MST, cCAT, and mCAT proteins were all detected in UAs of all three groups but did not differ among groups (Figure 3). These data show that human UA CBS, but not CSE, mRNA and protein expression are elevated during the proliferative phase of the menstrual cycle and pregnancy, two of the estrogen-dominant physiological states in women [35].
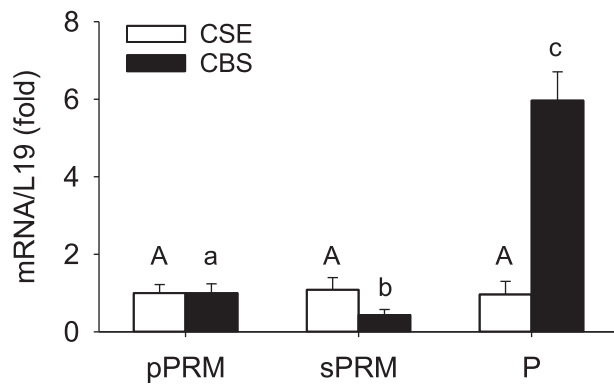
Figure 2. Effects of the menstrual cycle and pregnancy on CBS and CSE mRNAs in human UAs. Intact UA CBS and CSE mRNA were determined by real-time q-PCR. pPRM and sPRM: proliferative and secretory phases of the menstrual cycle; P: pregnancy. Data (mean ± SEM) are from 10 subjects/group. Bars with different letters differ significantly among the groups ($P < 0.001$).

Localization of cystathionine-beta-synthase and cystathionine-gamma-lyase proteins in human uterine artery

Immunofluorescence microscopic analysis revealed that CBS and CSE proteins were expressed in the intima (containing CD31-positive endothelial cells) and media (containing CD31-negative smooth muscle cells) in UAs of all three groups (Figure 4). CBS protein was localized in the endothelial cells at the apical surface of UA intima in all three groups, and its levels were in a rank order of P > NP pPRM > sPRM UAs ($P < 0.05$). The immunofluorescence staining of CBS was low in the media of NP sPRM UAs and significantly increased in NP pPRM UAs. Moreover, pregnancy further enhanced medial CBS protein expression by 6.45 ± 1.43-fold to that of NP pPRM UAs ($P < 0.05$). CSE immunofluorescence labeling was also observed at the apical surface and basement membrane of UA intima and throughout the smooth muscle cells of the UA media, but did not differ among groups. Thus, these data agree with the immunoblotting data (Figure 3) and also show that CBS, but not CSE, protein is upregulated in human UA endothelium and smooth muscle in estrogen-dominant physiological states.
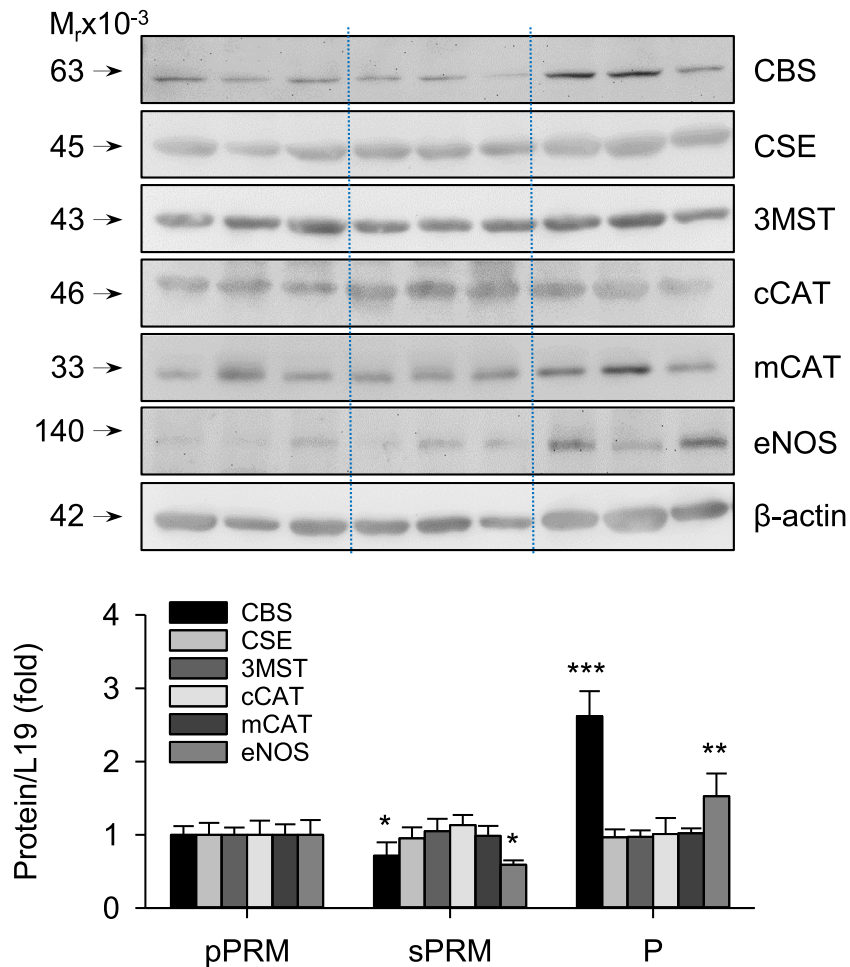

Figure 3. Effects of the menstrual cycle and pregnancy on H_2S biosynthesizing proteins in human UAs. CBS, CSE, NOS3, 3MST, cCAT, and mCAT protein was determined by immunoblotting. pPRM and sPRM: proliferative and secretory phases of the menstrual cycle; P: pregnancy. Data (mean ± SEM) are from 10 subjects/group. $*P < 0.05$, $**P < 0.01$, $***P < 0.001$, vs. pPRM.
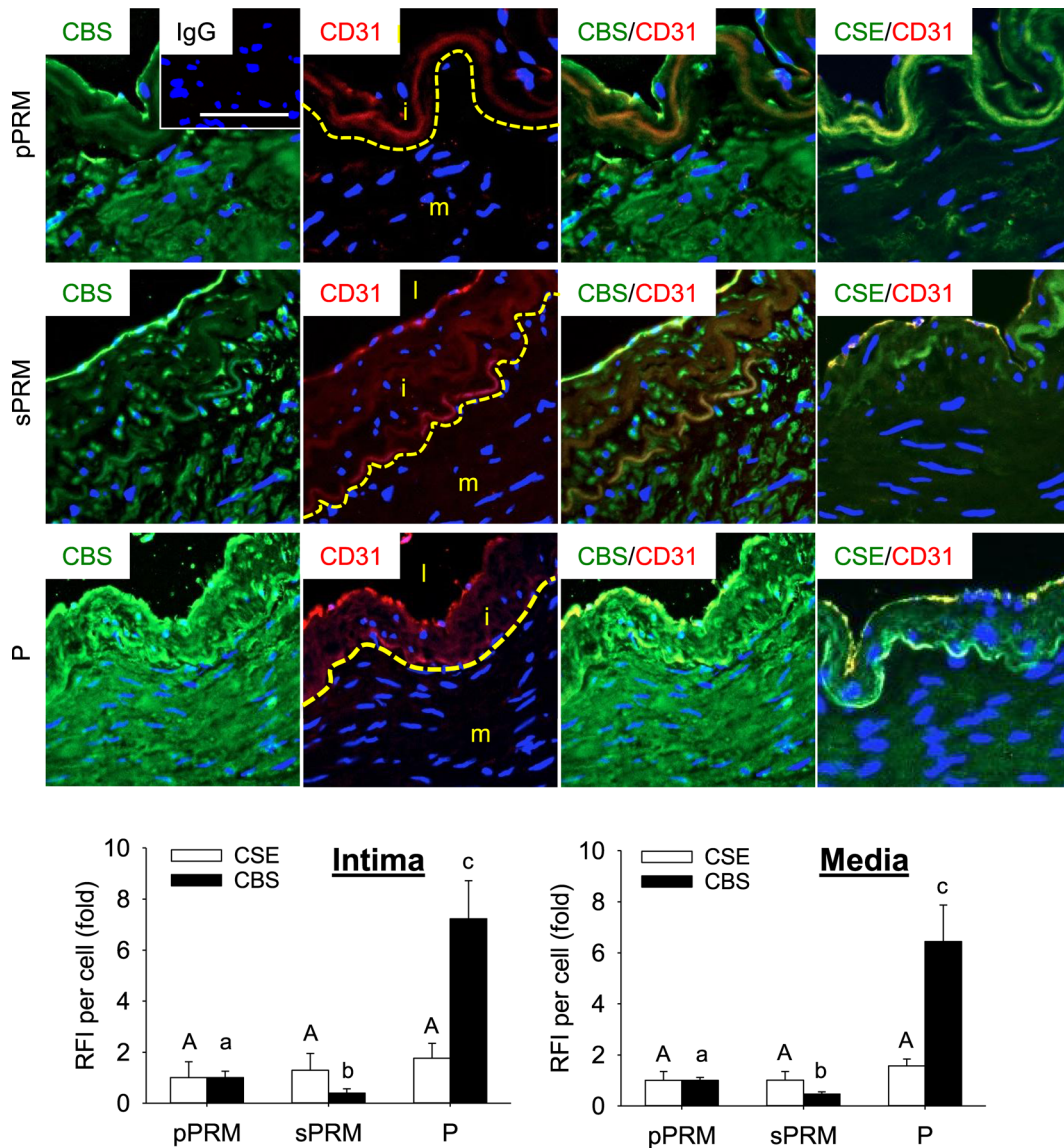
Figure 4. Effects of the menstrual cycle and pregnancy on CBS and CSE protein localization in human UAs. Uterine artery sections were labeled with primary antibodies against CBS or CSE, followed by secondary Alex^{486} (green)-labeled secondary antibody. Endothelial cells were labeled with marker CD31 followed by Alex^{586} (red)-labeled secondary antibody and cell nuclei were stained with DAPI (blue). Fluorescence images were captured for analyzing relative green fluorescence intensity (RFI) to quantify CBS or CSE proteins. pPRM and sPRM: proliferative and secretory phases of the menstrual cycle; P: pregnancy. Representative outlines of borders between UA intima and media were indicated, and UA lumen (l), intima (i), and media (m) were denoted (second panel). Data (mean ± SEM) are from 10 different subjects/group. Bars with different letters differ significantly among the groups ($P < 0.05$). Scale bar = 25 um.

H₂S-induced vasodilation

Since pregnancy augments H₂S biosynthesis in human UAs, we employed ex vivo organ bath studies using myography to determine whether H₂S contributes to pregnancy-associated uterine vasodilation. A slow releasing H₂S donor GYY4137 significantly relaxed phenylephrine-preconstricted UAs from both P and NP rats in a dose-dependent manner ($P < 0.001$; Figure 5). However, the vasodilating effect of GYY4137 is significantly greater in P-UA vs. NP-UA, with pD2 values of 7.43 ± 0.02 and 5.97 ± 0.01 ($P < 0.001$), respectively. Notably, GYY4137 did not relax phenylephrine-preconstricted MAs from P rats (Table 1). Thus, H₂S dilates UA with significantly greater potency in P vs. NP state and has tissue-specific vasodilatory effects.

Discussion

We have recently shown that exogenous estrogens significantly enhanced UA H₂S production in ovariectomized NP ewes in vivo [33]. We now first show that human UA H₂S production is significantly greater in the proliferative phase of the menstrual cycle, a physiological state that is associated with elevated endogenous estrogens, compared to the secretory phase [35]. Moreover, human UA H₂S production is further augmented ∼2-fold during pregnancy when total circulating estrogen levels increase nearly 1000-fold compared to NP state [35]. Thus, this study has shown that human UA H₂S biosynthesis is augmented during the estrogen-dominant physiological states during the follicular phase and pregnancy.
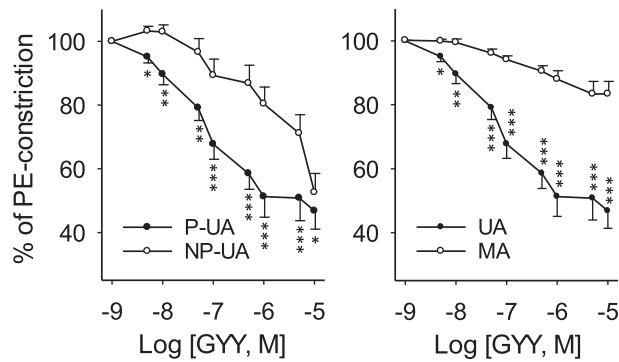
Figure 5. Effects of exogenous hydrogen sulfide (H_2S) on vasodilation. Endothelium intact primary uterine (UA, n = 12–18) and secondary mesenteric (MA, n = 12) arteries isolated from pregnant (P) (gestation day 20) and non-pregnant (NP) Sprague Dawley rats. Arteries were preconstricted with 10^{-6} M phenylephrine and exposed to a slow releasing H_2S donor GYY4137 (10^{-9}–10^{-5} M). $^*P < 0.05$, $^{**}P < 0.01$, and $^{***}P < 0.001$ for difference in the same dose.

Table 1. Potency of GYY4137 on relaxation of phenylephrine-preconstricted uterine (UA) and mesenteric (MA) arteries in non-pregnant (NP) and pregnant (P) rats.

Artery	n	pD2 value	P value
NP-UA	12–18	5.97 ± 0.01	<0.001
P-UA	12–18	$7.43 \pm 0.02^{***}$	<0.001
P-MA	12–18	ND	ND

$^{***}P < 0.001$ vs. NP-UA; $P < 0.001$ (ANOVA) vs. control for the same vessel; ND: non-detectable.

Endogenous H_2S in mammalian tissues is primarily synthesized from L-cysteine by two pyridoxal 5′-phosphate-dependent enzymes, including CBS and CSE [24, 25, 30]. Additionally, H_2S can be generated to a lesser extent by 3-MST that localizes to the cytosol or mitochondria to interact with CAT [26]. Our data shows that 3MST, cCAT, and mCAT proteins are expressed in human UA of all three groups and likely contributes to baseline H_2S in NP and P states. However, our data show that these enzymes do not account for changes of UA H_2S system as their protein expressions are not altered among different physiological states associated with different endogenous estrogens. Both CBS and CSE are needed to generate H_2S in some tissues, while in others one enzyme is sufficient [22, 36]. Therefore, the expression of CBS and CSE can be tissue and cell specific. CSE is found to be closely associated with vasculature tissue [30]. Although CBS is initially reported to be mainly expressed in neuronal tissue [21], it has also been found to be expressed in the cerebral arteries of newborn pigs [24] and pulmonary arteries of mice with decreased expression in a rat model of pulmonary hypertension [37]. We have recently shown in NP sheep UA basal CSE protein expression is high and basal CBS protein is low; however, CBS is the one that is responsive to estrogen stimulation in vivo [33]. Our current data show immunologically strong basal CSE protein expression with no difference in pPRM and sPRM NP and P human UAs. Weak baseline CBS protein is also immunologically detectable in sPRM human UAs; however, its levels are significantly increased in pPRM NP and P UAs. Furthermore, changes in UA CSE and CBS mRNAs match changes in their proteins among different physiological states, indicating that transcriptional mechanisms are involved in CBS expression associated with endogenous estrogens in the proliferative phase and pregnancy in human UA. In keeping with the changes in

circulating estrogen levels during the menstrual cycle and pregnancy in women [35] and a stimulatory effect of exogenous estrogens on CBS, but not CSE, expression in sheep UAs [33], our current study establishes a positive link between endogenous estrogens and CBS expression in human UA and that *CBS* is a pregnancy-responsive gene in the vascular wall.

Since CBS and CSE are expressed in human UA, both may contribute to basal UA H_2S production during the menstrual cycle and pregnancy. However, our data show that CBS is the major enzymatic pathway for pregnancy-augmented H_2S biosynthesis in human UA. Consistent with the aforementioned findings showing that CBS, but not CSE, mRNA and protein are increased in pPRM vs. sPRM NP UAs and further augmented in P UAs, it is highly likely that pregnancy-augmented UA H_2S biosynthesis in women is mediated by upregulating CBS expression possibly via transcriptional mechanisms, and linked to elevated endogenous estrogens that are synthesized locally in the placenta during pregnancy [38, 39].

The present data are collected from 20 NP UAs from hysterectomies with various medical complications and 10 P UAs from subjects with placenta accreta. With these samples we are able to repeat previously reported augmented NOS3 protein expression in human UA during estrogen-dominant physiological states [16]. This result validates the quality of the sample collection procedure. Since human primary UAs can be only collected in an event of hysterectomy, in general under disease conditions that may impact UA gene expression. A follow-up study with greater sample size is needed to stratify UA H_2S biosynthesis with different disease conditions.

Our current study is the first to show UA H_2S biosynthesis during the ovarian cycle and pregnancy. These findings obviously raise a key question as to what roles H_2S play in the UA. We believe that the physiological significance of pregnancy-augmented UA H_2S biosynthesis underlines a role of H_2S in mediating pregnancy-associated rise in UBF due to the potent vasodilatory [27] and angiogenic properties of H_2S [29]. Indeed, we have shown in this study that a slow releasing H_2S donor GYY4137 more efficiently relaxes primary UAs from P vs. NP rats. Although this finding shows that exogenous H_2S can relax P UAs and thus, may be associated with uterine physiology in pregnancy, further studies are needed to delineate if blockade of endogenous H_2S biosynthesis attenuates pregnancy-associated uterine vasodilation. In animal models, pregnancy and estrogens stimulate the expression and activation of UA BK_{Ca} [40, 41]. BK_{Ca} channels contribute to vascular function in NP human UA [42] and the rise and maintenance of estrogen-induced uterine vasodilation and maintenance of blood pressure in ewes [43]. Pregnancy also regulates K_{ATP} channels that are important in pregnancy- and hypoxia-regulated UA vascular tone in ewes [44]. Thus, we speculate that endogenous H_2S plays an important role in uterine vasodilation as these pregnancy- and estrogen-responsive K^+ channels are the major signaling pathways that mediate the vascular effects of H_2S [21, 27, 45]. Interestingly, exogenous H_2S appears to have tissue-specific effects since GYY4137 did not relax systemic MAs from P rats. This is also seen with changes in the BK_{Ca} channel expression after estrogen exposure [40]. To this end, further studies are warranted to explore if H_2S has a role in systemic vascular adaptation to pregnancy as well.

In a tube-shaped large human artery like UA, the luminal surface intima containing a thin layer of endothelial cells covers the media composed of a thick layer of smooth muscle cells. Our immunofluorescence microscopy studies have revealed that both endothelium and smooth muscle express CBS and CSE and their levels mirror the protein expression patterns revealed by immunoblotting. In the

vascular wall, endothelial cells produce the other well-documented vasodilator NO synthesized by NOS3 [46]; in the UA, NO is believed to be exclusively produced by NOS3 expressed mainly in the endothelium [12]. Endothelium-derived NO plays a key role in UA smooth muscle remodeling [17, 18] and contributes to relaxation/dilation during pregnancy [9]. Our current data show that both endothelium and smooth muscle contribute to H_2S biosynthesis in human UA, similar to our recent animal studies [33]. In keeping with the facts that H_2S activates NOS3 in endothelial cells during in vitro and in vivo angiogenesis [29], localization of CBS and CSE protein and pregnancy-dependent CBS and CSE expression in both cell types suggest that H_2S may function as a key mediator for regulating smooth muscle-endothelial cell interactions in the UA. This idea, if proven, will reshape the understanding of how endothelium interacts with smooth muscle on vessel wall in a two-way fashion that not only can the endothelium regulate smooth muscle function via NO but also smooth muscle can regulate endothelium function via H_2S.

In summary, our present study shows for the first time that augmented H_2S biosynthesis due to enhanced endothelium and smooth muscle CBS mRNA and protein expression is linked to elevated endogenous circulating estrogens during the follicular phase of the menstrual cycle and pregnancy, contributing to pregnancy-associated uterine vasodilation. However, it is needed to point out that although our recent reports (33 and the current study) have pioneered a potential critical role of H_2S in uterine hemodynamics physiology, there is much more knowledge that needs to be learned before a throughout elucidation of a role that H_2S may play in uterine hemodynamics dysregulation can be determined.

Supplementary data

Supplementary data are available at *BIOLRE* online.

References

1. Osol G, Mandala M. Maternal uterine vascular remodeling during pregnancy. *Physiology (Bethesda)* 2009; **24**:58–71.
2. Rosenfeld CR. Distribution of cardiac output in ovine pregnancy. *Am J Physiol* 1977; **232**:H231–H235.
3. Carr DJ, Wallace JM, Aitken RP, Milne JS, Martin JF, Zachary IC, Peebles DM, David AL. Peri- and postnatal effects of prenatal adenoviral VEGF gene therapy in growth-restricted sheep. *Biol Reprod* 2016, **94**:142–153.
4. Reynolds LP, Caton JS, Redmer DA, Grazul-Bilska AT, Vonnahme KA, Borowicz PP, Luther JS, Wallace JM, Wu G, Spencer TE. Evidence for altered placental blood flow and vascularity in compromised pregnancies. *J Physiol* 2006; **572**:51–58.
5. Romero R, Dey SK, Fisher SJ. Preterm labor: one syndrome, many causes. *Science* 2014; **345**:760–765.
6. Barker DJ. Intrauterine programming of adult disease. *Mol Med Today* 1995; **1**:418–423.
7. Fitzgerald DJ, Entman SS, Mulloy K, FitzGerald GA. Decreased prostacyclin biosynthesis preceding the clinical manifestation of pregnancy-induced hypertension. *Circulation* 1987; **75**:956–963.
8. Majed BH, Khalil RA. Molecular mechanisms regulating the vascular prostacyclin pathways and their adaptation during pregnancy and in the newborn. *Pharmacol Rev* 2012; **64**:540–582.
9. Rosenfeld CR, Cox BE, Roy T, Magness RR. Nitric oxide contributes to estrogen-induced vasodilation of the ovine uterine circulation. *J Clin Invest* 1996; **98**:2158–2166.
10. Gokina NI, Kuzina OY, Vance AM. Augmented EDHF signaling in rat uteroplacental vasculature during late pregnancy. *Am J Physiol Heart Circ Physiol* 2010; **299**:H1642–H1652.
11. Ni Y, May V, Braas K, Osol G. Pregnancy augments uteroplacental vascular endothelial growth factor gene expression and vasodilator effects. *Am J Physiol* 1997; **273**:H938–H944.
12. Vagnoni KE, Shaw CE, Phernetton TM, Meglin BM, Bird IM, Magness RR. Endothelial vasodilator production by uterine and systemic arteries. III. Ovarian and estrogen effects on NO synthase. *Am J Physiol* 1998; **275**:H1845–H1856.
13. Chen DB, Bird IM, Zheng J, Magness RR. Membrane estrogen receptor-dependent extracellular signal-regulated kinase pathway mediates acute activation of endothelial nitric oxide synthase by estrogen in uterine artery endothelial cells. *Endocrinology* 2004; **145**:113–125.
14. Chen DB, Jia S, King AG, Barker A, Li SM, Mata-Greenwood E, Zheng J, Magness RR. Global protein expression profiling underlines reciprocal regulation of caveolin 1 and endothelial nitric oxide synthase expression in ovariectomized sheep uterine artery by estrogen/progesterone replacement therapy. *Biol Reprod* 2006; **74**:832–838.
15. Nelson SH, Steinsland OS, Suresh MS, Lee NM. Pregnancy augments nitric oxide-dependent dilator response to acetylcholine in the human uterine artery. *Hum Reprod* 1998; **13**:1361–1367.
16. Nelson SH, Steinsland OS, Wang Y, Yallampalli C, Dong YL, Sanchez JM. Increased nitric oxide synthase activity and expression in the human uterine artery during pregnancy. *Circ Res* 2000; **87**:406–411.
17. van der Heijden OW, Essers YP, Fazzi G, Peeters LL, De Mey JG, van Eys GJ. Uterine artery remodeling and reproductive performance are impaired in endothelial nitric oxide synthase-deficient mice. *Biol Reprod* 2005; **72**:1161–1168.
18. Kulandavelu S, Whiteley KJ, Qu D, Mu J, Bainbridge SA, Adamson SL. Endothelial nitric oxide synthase deficiency reduces uterine blood flow, spiral artery elongation, and placental oxygenation in pregnant mice. *Hypertension*; **60**:231–238.
19. Itoh S, Brawley L, Wheeler T, Anthony FW, Poston L, Hanson MA. Vasodilation to vascular endothelial growth factor in the uterine artery of the pregnant rat is blunted by low dietary protein intake. *Pediatr Res* 2002; **51**:485–491.
20. Rosenfeld CR, Roy T. Prolonged uterine artery nitric oxide synthase inhibition modestly alters basal uteroplacental vasodilation in the last third of ovine pregnancy. *Am J Physiol Heart Circ Physiol* 2014; **307**:H1196–H1203.
21. Wang R. Physiological implications of hydrogen sulfide: a whiff exploration that blossomed. *Physiol Rev* 2012; **92**:791–896.
22. Gadalla MM, Snyder SH. Hydrogen sulfide as a gasotransmitter. *J Neurochem* 2010; **113**:14–26.
23. Mustafa AK, Gadalla MM, Sen N, Kim S, Mu W, Gazi SK, Barrow RK, Yang G, Wang R, Snyder SH. H_2S signals through protein S-sulfhydration. *Sci Signal* 2009; **2**:ra72.
24. Leffler CW, Parfenova H, Basuroy S, Jaggar JH, Umstot ES, Fedinec AL. Hydrogen sulfide and cerebral microvascular tone in newborn pigs. *Am J Physiol Heart Circ Physiol* 2011; **300**:H440–H447.
25. Bhatia M. Hydrogen sulfide as a vasodilator. *IUBMB Life* 2005; **57**:603–606.
26. Shibuya N, Mikami Y, Kimura Y, Nagahara N, Kimura H. Vascular endothelium expresses 3-mercaptopyruvate sulfurtransferase and produces hydrogen sulfide. *J Biochem* 2009; **146**:623–626.
27. Zhao W, Zhang J, Lu Y, Wang R. The vasorelaxant effect of H_2S as a novel endogenous gaseous K_{ATP} channel opener. *EMBO J* 2001; **20**:6008–6016.
28. Li Y, Zang Y, Fu S, Zhang H, Gao L, Li J. H_2S relaxes vas deferens smooth muscle by modulating the large conductance Ca^{2+}-activated K^+ (BK_{Ca}) channels via a redox mechanism. *J Sex Med* 2012; **9**:2806–2813.
29. Papapetropoulos A, Pyriochou A, Altaany Z, Yang G, Marazioti A, Zhou Z, Jeschke MG, Branski LK, Herndon DN, Wang R, Szabo C. Hydrogen sulfide is an endogenous stimulator of angiogenesis. *Proc Natl Acad Sci USA* 2009; **106**:21972–21977.
30. Yang G, Wu L, Jiang B, Yang W, Qi J, Cao K, Meng Q, Mustafa AK, Mu W, Zhang S, Snyder SH, Wang R. H_2S as a physiologic vasorelaxant: hypertension in mice with deletion of cystathionine gamma-lyase. *Science* 2008; **322**:587–590.

31. Cindrova-Davies T. The therapeutic potential of antioxidants, ER chaperones, NO and H$_2$S donors, and statins for treatment of preeclampsia. *Front Pharmacol* 2014; **5**:119.

32. Wang K, Ahmad S, Cai M, Rennie J, Fujisawa T, Crispi F, Baily J, Miller MR, Cudmore M, Hadoke PW, Wang R, Gratacos E et al. Dysregulation of hydrogen sulfide producing enzyme cystathionine gamma-lyase contributes to maternal hypertension and placental abnormalities in preeclampsia. *Circulation* 2013; **127**:2514–2522.

33. Lechuga TJ, Zhang HH, Sheibani L, Karim M, Jia J, Magness RR, Rosenfeld CR, Chen DB. Estrogen replacement therapy in ovariectomized nonpregnant ewes stimulates uterine artery hydrogen sulfide biosynthesis by selectively up-regulating cystathionine beta-synthase expression. *Endocrinology* 2015; **156**:2288–2298.

34. Chinnathambi V, Blesson CS, Vincent KL, Saade GR, Hankins GD, Yallampalli C, Sathishkumar K. Elevated testosterone levels during rat pregnancy cause hypersensitivity to angiotensin II and attenuation of endothelium-dependent vasodilation in uterine arteries. *Hypertension* 2014; **64**:405–414.

35. O'Leary P, Boyne P, Flett P, Beilby J, James I. Longitudinal assessment of changes in reproductive hormones during normal pregnancy. *Clin Chem* 1991; **37**:667–672.

36. Mustafa AK, Gadalla MM, Snyder SH. Signaling by gasotransmitters. *Sci Signal* 2009; **2**:re2.

37. Chertok VM, Kotsyuba AE. Distribution of H$_2$S synthesis enzymes in the walls of cerebral arteries in rats. *Bull Exp Biol Med* 2012; **154**:104–107.

38. Albrecht ED, Pepe GJ. Placental steroid hormone biosynthesis in primate pregnancy. *Endocr Rev* 1990; **11**:124–150.

39. Magness RR, Rosenfeld CR. The role of steroid hormones in the control of uterine blood flow. In: *The Uterine Circulation*, vol 10. Ithaca, NY: Perinatology Press, 1989; 239–271.

40. Rosenfeld CR, Liu XT, DeSpain K. Pregnancy modifies the large conductance Ca^{2+}-activated K$^+$ channel and cGMP-dependent signaling pathway in uterine vascular smooth muscle. *Am J Physiol Heart Circ Physiol* 2009; **296**:H1878–H1887.

41. Nagar D, Liu XT, Rosenfeld CR. Estrogen regulates beta-subunit expression in Ca^{2+}-activated K$^+$ channels in arteries from reproductive tissues. *Am J Physiol Heart Circ Physiol* 2005; **289**:H1417–H1427.

42. Rosenfeld CR, Word RA, DeSpain K, Liu XT. Large conductance Ca^{2+}-activated K$^+$ channels contribute to vascular function in nonpregnant human uterine arteries. *Reprod Sci* 2008; **15**:651–660.

43. Rosenfeld CR, Cornfield DN, Roy T. Ca^{2+}-activated K$^+$ channels modulate basal and E2beta-induced rises in uterine blood flow in ovine pregnancy. *Am J Physiol Heart Circ Physiol* 2001; **281**:H422–H431.

44. Xiao D, Longo LD, Zhang L. Role of KATP and L-type Ca^{2+} channel activities in regulation of ovine uterine vascular contractility: effect of pregnancy and chronic hypoxia. *Am J Obstet Gynecol* 2010; **203**:596 e596–512.

45. Hersperger R, Buchheit KH, Cammisuli S, Enz A, Lohse O, Ponelle M, Schuler W, Schweitzer A, Walker C, Zehender H, Zenke G, Zimmerlin AG et al. A locally active antiinflammatory macrolide (MLD987) for inhalation therapy of asthma. *J Med Chem* 2004; **47**:4950–4957.

46. Forstermann U, Munzel T. Endothelial nitric oxide synthase in vascular disease: from marvel to menace. *Circulation* 2006; **113**:1708–1714.